International Journal of Informatics and Communication Technology (IJ-ICT)
Vol. 15, No. 2, June 2026, pp. 508∼522
ISSN: 2252-8776, DOI: 10.11591/ijict.v15i2.pp508-522

A robust outlier detection based filtering for noise removal in grayscale images

Ali Salem Al Rawash[1], Farah Aini Abdullah[1], Ahmad Kadri Junoh[2], Abdallah Alshbeel[1], Mohammed Banikhalid[1]
[1]School of Mathematical Sciences, University Sains Malaysia Gelugor, Penang, Malaysia
[2]Faculty of Intelligent Computing, Universiti Malaysia Perlis, Arau, Malaysia

Article Info

Article history:

Received Jul 11, 2025
Revised Mar 4, 2026
Accepted Mar 30, 2026

Keywords:

Image denoising
Image restoration
Interquartile range
Outlier detection
Salt and pepper noise

ABSTRACT

Salt-and-pepper noise severely degrades the visual quality of digital images, particularly at high noise densities where conventional denoising techniques often fail. Median- and mean-based filters tend to oversmooth images and blur fine structures when the majority of pixels within a local window are corrupted. This paper proposes a robust dual-layer denoising framework for grayscale images that integrates rank-based prescreening, interquartile range (IQR)-based statistical outlier detection using Tukey fences, and a lightweight post-processing sharpening stage. In the first layer, a rank-4 trimmed estimator suppresses extreme impulse values and stabilizes local statistics. In the second layer, adaptive IQR thresholds are employed to detect and replace residual outliers, even in heavily corrupted neighborhoods. A final step involving selective sharpening combined with mild smoothing enhances edge details without amplifying residual noise. Extensive experiments on standard grayscale images (Lenna, Barbara, lake, boat, and living room) across salt-and-pepper noise levels from 10% to 90% demonstrate that the proposed approach consistently outperforms conventional methods, including mean, median, Gaussian, modified decision based unsymmetrical trimmed median filter (MDBUTMF), and pixel density-based filter (BPDF). Quantitative evaluation indicates peak signal-to-noise ratio (PSNR) values reaching 38.23dB, structural similarity index (SSIM) values up to 0.99, and significant reductions in mean squared error (MSE), particularly at higher noise densities. These results confirm that the proposed framework effectively suppresses noise while preserving edges and textures, making it well-suited for practical applications such as medical imaging, remote sensing, and surveillance.

Corresponding Author:

Ahmad Kadri Junoh
Faculty of Intelligent Computing, University Malaysia Perlis
Arau, Malaysia
Email: kadri@unimap.edu.my

1. INTRODUCTION

Noise reduction remains a fundamental problem in digital image processing despite decades of research [1]. Digital images are representations of real-world scenes captured through digital sensors and stored as pixel matrices [2]. Each pixel encodes intensity information, and damage to these pixels-such as through noise contamination-can degrade image quality and hinder analysis. Image processing techniques aim to restore or enhance image quality, often through filtering methods that suppress noise while preserving important

structural features [3], [4]. Effective noise removal is crucial in image processing, but it must be achieved without compromising essential image information. Satpathy *et al*. [5] Accurate restoration of corrupted image intensities while preserving structural details remains a significant challenge. Numerous techniques have been employed for image denoising [6]. Salt-and-pepper noise, typically resulting from abrupt disturbances such as sensor faults or transmission errors, leads to significant degradation in image quality. Although notable progress has been made in mitigating salt and pepper noise, challenges like image blurring and structural distortion continue to hinder performance. Thus, there remains a pressing need to improve the effectiveness and precision of denoising techniques [7].

A major challenge in image processing is mitigating high-density salt-and-pepper noise, a type of impulsive corruption in which affected pixels assume either minimum (0) or maximum (255) intensity values [8]. This noise disrupts local image statistics, causing structural distortions and loss of fine details. Critical applications-including medical imaging, remote sensing, and surveillance-require robust denoising techniques that can restore visual clarity while preserving structural integrity [9], [10].

Numerous denoising techniques have been proposed. Median-based filters such as the median filter (MF) and its variants (weighted median, adaptive median) that performing well at low-to-moderate noise densities by preserving edges while removing outliers [11], [12]. However, at higher noise levels (typically above 50%, these methods suffer from excessive smoothing, misclassification of valid pixels, and loss of fine details [13]. Advanced denoising methods aim to remove noise while preserving textures and edges. Some approaches utilize partial differential equations (PDEs), such as anisotropic second- and fourth-order diffusion models based on convolutional virtual electric fields and gradient vector convolution [14]. Additionally, the median filter remains relevant in modern noise removal techniques, often in modified forms or combined with other methods. Examples include the tropical MF (TMF), different applied MF (DAMF), based pixel density filter (BPDF), modified decision-based unsymmetric trimmed median filter, adaptive fuzzy switching median filter, and tropical adaptive filter [15].

Several studies have attempted to address these limitations through adaptive or weighted strategies, such as the tropical median filter and decision-based filters, provide incremental improvements; however, their performance degrades significantly when noise density exceeds 60% [16]. Digitally acquired images are frequently degraded by noise, which not only reduces visual quality but also influences human visual perception. In response, PDE-based models have emerged in recent years as effective denoising tools, offering the key advantage of reducing noise while preserving essential image details [17]. Conventional outlier detection techniques construct a model of the data and classify points that deviate markedly as outliers. However, when the dataset contains a high proportion of outliers, these anomalous points can distort the model itself, reducing its reliability and causing most standard detectors to fail [18].

Despite these advancements, a gap remains: existing techniques either excessively smooth the image, fail at high noise densities, or require impractical computational resources. This study aims to develop a robust, efficient denoising method for grayscale images with high-density salt-and-pepper noise. The proposed technique integrates adaptive rank filtering, statistical outlier detection (using the interquartile range), and image sharpening to achieve superior noise suppression while preserving structural details and fine textures.

A hybrid denoising method is proposed to combine rank filtering and interquartile range (IQR)-based outlier detection tailored for high-density salt-and-pepper noise in grayscale images. Limitations of existing median-based and PDE-based filters are critically analyzed to show how proposed method overcomes these challenges. An image sharpening stage that restores fine details without amplifying residual noise are introduced. Then, the method across standard test images and demonstrate superior performance over traditional techniques in terms of peak signal-to-noise ratio (PSNR), structural similarity index (SSIM), and mean squared erro (MSE) are validated. Although rank-based, switching, and quartile-driven filters have been individually explored, no existing denoising approach integrates,

- Rank-4 trimmed prescreening
- Adaptive Tukey-fence outlier detection (IQR-based)
- Sharpening guided by statistically cleaned estimates

The novelty of the proposed method lies in the synergistic combination of these three elements. Rank-4 reduces extreme impulses, IQR-based statistics enable adaptive outlier detection even in heavily corrupted windows, and sharpening restores details suppressed by median operations. This hybrid design produces exceptional robustness, sustaining performance up to 80–90% noise density, far beyond the limits of traditional filters.

2. RELATED WORKS

Over the past decades, numerous image restoration techniques have been developed to address salt-and-pepper noise contamination. Despite these advances, many existing approaches demonstrate notable performance degradation at elevated noise densities, particularly when the corruption level exceeds approximately 60–70%, where maintaining structural integrity and fine details becomes increasingly challenging [19]. Among classical solutions, median-based filtering techniques remain widely adopted due to their simplicity and effectiveness against impulsive noise. The standard MF replaces each pixel with the median value of its surrounding neighborhood, which enables effective suppression of isolated outliers at low to moderate noise levels. However, when the noise density surpasses roughly 50%, MF exhibits excessive smoothing behavior, leading to edge blurring and significant loss of high-frequency image details [20].

To overcome these limitations, several enhanced median-based approaches have been proposed. One such method is the Adaptive Wiener Filter, which incorporates two-dimensional maximum Shannon entropy to improve denoising stability under high-density noise conditions [21]. Although this approach demonstrates improved suppression of impulsive noise, its effectiveness remains limited in images with complex textures and structural variations, indicating the need for further refinement. In another study, a real-time denoising framework employing double-nested filtering combined with morphological dilation was introduced to remove high-density salt-and-pepper noise in medical imaging applications [22]. Iterative filtering strategies have also been explored, such as the iterative MF (IMF), which estimates corrupted pixels using the mean intensity of detected noise-free pixels within a fixed window [23]. Although IMF performs satisfactorily at low noise densities, its reliability deteriorates as noise density increases, since the number of valid pixels available for accurate estimation rapidly diminishes. Other notable techniques include the adaptive MF (AMF), which dynamically adjusts the window size according to local noise conditions [24].

While AMF improves upon the conventional MF, it may inadvertently modify uncorrupted pixels, resulting in degradation of fine image features and edge structures. At noise densities exceeding 60%, AMF increasingly misclassifies clean pixels as noisy, leading to structural distortion [25]. Several variants, such as the weighted MF (WMF) and the progressive switching MF (PSMF), have been proposed to reduce unnecessary smoothing and enhance detail preservation. Nevertheless, these methods continue to face significant challenges under extreme noise conditions, as their noise detection accuracy declines substantially at high corruption levels [26].

Beyond median-based techniques, PDE-based methods, including anisotropic diffusion and total variation models, have been applied to salt-and-pepper noise removal. These approaches aim to preserve edge information while smoothing noise through iterative diffusion processes. Although effective in maintaining structural continuity, PDE-based methods often suffer from blurring artifacts at high noise densities and require careful parameter tuning, which limits their suitability for real-time or computationally constrained environments [27].

Despite the development of these diverse filtering strategies, a persistent challenge remains: balancing noise removal with the preservation of fine image details in the presence of high-density salt-and-pepper noise. The proposed method in this study addresses this gap by combining rank filtering, statistical outlier detection using interquartile range analysis, and image sharpening. This hybrid approach is designed to provide superior noise suppression while maintaining structural integrity, particularly in grayscale images affected by extreme noise conditions.

Existing filters degrade severely when the number of corrupted pixels exceeds the number of clean pixels in the neighborhood. They rely on fixed rules or trimmed medians rather than adaptive statistical boundaries. The proposed method fills this gap by incorporating rank statistics + IQR statistics, enabling reliable outlier detection even in heavily corrupted windows.

3. PROPOSED METHOD

This section introduces the proposed dual-layer denoising framework designed to remove high-density salt-and-pepper noise from grayscale images. The Algorithm consists of three main components: (i) rank-based prescreening, (ii) IQR-based statistical outlier detection, and (iii) sharpening with mild smoothing. All operations are applied locally on 3×3 neighborhoods. Comparison of key features between existing filters and the proposed method in Table 1.

3.1. Local window and notation

For each pixel I(x,y), a fixed 3×3 local window is extracted,

$$W(x,y) = \{I(i,j) \mid i \in [x-1, x+1], j \in [y-1, y+1]\}$$

The nine values in the window are sorted in ascending order,

$$S = \{p_1 \leq p_2 \leq p_3 \leq p_4 \leq p_5 \leq p_6 \leq p_7 \leq p_8 \leq p_9\}$$

Table 1. Comparison of key features between existing filters and the proposed method

Method	Rank filt.	IQR stat.	Switch logic	Noise >70%	Edge pres.	Notes
Median filter	No	No	No	No	No	Fails when most pixels in the window are noisy.
AMF	No	No	Yes	∼60%	No	Variable window; unstable at very high noise levels.
BPDF	No	No	Yes	∼70%	No	Performance degrades when clean pixels are scarce.
MDBUTMF	No	No	Yes	∼70%	No	Trims extreme values; still dependent on fixed decision rules.
Proposed	Yes	Yes	Yes	Yes	Yes	Dual-layer hybrid method with statistical adaptivity.

3.2. Layer 1: Rank-based prescreening (Rank = 4)

Salt-and-pepper noise introduces extreme values that distort the local statistics. To reduce their influence, a rank-4 value is used as a trimmed estimator,

$$R = p_4$$

Let the center pixel be $w_c = I(x,y)$. The prescreening rule is,

$$I_1(x,y) = \begin{pmatrix} R, & if\ is\ inconsistent\ with\ R \\ w_c & otherwise. \end{pmatrix}$$

Where,
- $I_1(x,y)$: output of the prescreening layer
- $R = p_4$: rank-4 robust estimate
- w_c : center pixel

Rank-4 filtering stabilizes the local distribution and reduces strong impulses before the statistical detection stage.

3.3. Layer 2: IQR-based statistical outlier detection (1.5 × IQR)

The second layer performs adaptive outlier detection using quartile statistics derived from the sorted window S.

- Quartiles,

$$Q_1 = p_3, \quad Q_3 = p_7$$

- Interquartile Range,

$$IQR = Q_3 - Q_1 \tag{1}$$

- Tukey Fences ($1.5 \times IQR$),

$$LOL = Q_1 - 1.5IQR \tag{2}$$

$$UOL = Q_3 + 1.5IQR \tag{3}$$

A value v in the window is declared an outlier if,

$$v < LOL \quad \text{or} \quad v > UOL$$

All detected outliers are replaced with the median,

$$v \leftarrow p_5$$

The corrected center pixel after this layer is written as,

$$I_2(x, y) = p_5$$
$$I_{\text{final}} = G_\sigma(I_{\text{sharp}}), \quad \sigma \approx 0.5$$
$$W(x, y) = \{I(i, j) \mid i \in [x-1, x+1], j \in [y-1, y+1]\}$$

Where,
- Q_1, Q_3 : first and third quartiles
- IQR: interquartile range.
- LOL, UOL: lower and upper Tukey limits.
- p_5: original median.
- p_5* : corrected median after outlier replacement.
- $I_2(x, y)$: IQR-corrected output pixel.

The median p_5 appears in two stages,
- In Layer 1, p_5 is implicitly related to p_4, since rank-4 lies close to the median and helps stabilize the distribution.
- In Layer 2, p_5 is explicitly used to replace statistical outliers because it is the most robust estimate against impulse noise.

Thus, the median supports stability in Layer 1 and robust replacement in Layer 2, each serving a different function.

3.4. Post-denoising sharpening and smoothing

Median-based operations may slightly smooth edges. To restore edge sharpness, a linear unsharp-masking operator is applied,

Where,

I_1: prescreened image
I_2: IQR-corrected image
1.5: enhances high-frequency edge components
-0.5: subtracts part of the smoothed component
-0.5: intensity shift maintaining numerical stability

A mild Gaussian blur is then applied:

$$I_{\text{final}} = G_\sigma(I_{\text{sharp}}), \quad \sigma \approx 0.5$$

where G_σ denotes convolution with a Gaussian kernel.

Rationale for the chosen weights,
- 1.5 amplifies edges without producing ringing artifacts (values above 2 cause overshoot).
- 1.5 amplifies edges without producing ringing artifacts (values above 2 cause overshoot).
- –0.5 (bias) ensures the weighted sum remains within the valid intensity range
- $\sigma \approx 0.5$ provides gentle smoothing that reduces sharpening noise.

3.5. Performance metrics

The performance of the proposed method is assessed using three standard image quality metrics: PSNR, MSE, and SSIM. PSNR quantifies the fidelity of the reconstructed image relative to the reference image, where higher values indicate superior reconstruction quality, and is defined as,

$$PSNR = 10log_{10}(\frac{MAX^2}{MSE}) \tag{4}$$

Where, MAX represents the maximum possible pixel value (255 for 8-bit images), and MSE is the mean squared error. MSE quantifies the average squared difference between the original and processed images,

$$MSE = \frac{1}{n}\sum_{i=1}^{n}(Y_i - \widehat{Y}_i)^2 \tag{5}$$

The MSE is calculated by taking the sum of the squared differences between the observed values (Yi) and the predicted values (Y), divided by the number of data points (n). The SSIM formula is computed as follows,

$$SSIM = \frac{(2\mu_x\mu_y + C_1) + (2\sigma_{xy} + C_2)}{(\mu_x^2 + \mu_y^2 + C_1) + (\sigma_x^2 + \sigma_y^2 + C_2)} \tag{6}$$

μ_x and μ_y represent the average intensities (standard deviation) in the x and y directions, respectively. The SSIM value is kept at one using constants C_1 and C_2. These metrics are computed for each iteration, and the results are recorded for further analysis. The final output is expected to show significant improvement in image quality with reduced noise and preserved detail.

3.6. Pseudocode

The Algorithm 1 consists of three main components: (i) rank- based prescreening, (ii) IQR-based statistical outlier detection, and (iii) sharpening with mild smoothing.

Algorithm 1: Proposed hybrid denoising algorithm

Input : Noisy grayscale image I
Output: Final denoised image I_{final}

for *each pixel* (x, y) **do**
  Extract $W = 3 \times 3$ window
  Sort $W \rightarrow \{p_1 \leq p_2 \leq \cdots \leq p_9\}$
  `// Layer 1: Rank-based prescreening`
  $R \leftarrow p_4$
  if *center pixel deviates from* R **then**
    $I_1(x, y) \leftarrow R$
  else
    $I_1(x, y) \leftarrow$ center pixel
  `// Layer 2: IQR-based outlier detection`
  Recompute sorted window if needed
  $Q_1 \leftarrow p_3, \quad Q_3 \leftarrow p_7$
  $IQR \leftarrow Q_3 - Q_1$
  $LOL \leftarrow Q_1 - 1.5 \times IQR$
  $HOL \leftarrow Q_3 + 1.5 \times IQR$
  foreach *value* v *in* W **do**
    if $v < LOL$ ***or*** $v > HOL$ **then**
      $v \leftarrow p_5$
  $I_2(x, y) \leftarrow$ corrected center value
`// Sharpening and Smoothing`
$I_{sharp} \leftarrow 1.5 \times I_1 - 0.5 \times I_2 - 0.5$
$I_{final} \leftarrow$ GaussianBlur$(I_{sharp}, 3 \times 3, \sigma \approx 0.5)$

3.7. Flowchart of the proposed method

Flowchart illustrating the proposed dual-layer denoising framework, including rank-4 prescreening, IQR-based outlier removal ($1.5 \times IQR$ Tukey fences) [28]-[30], and the sharpening–smoothing post-processing stage and it shown in Figure 1.

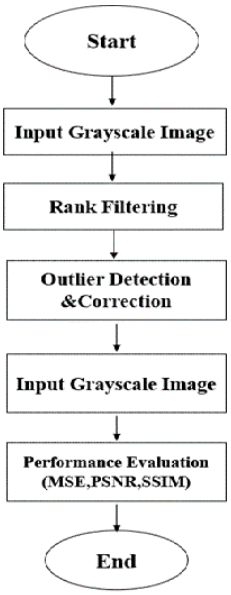

Figure 1. Flowchart for the method

4. RESULT AND DISCUSSION

4.1. Experimental setup

All experiments were implemented in Python using NumPy, SciPy, Pillow, and scikit-image libraries. The proposed method was applied on a fixed 3×3 window, using replicate padding for boundary handling. The rank-4 prescreening and $1.5 \times IQR$ Tukey fences remained constant for all test images. Synthetic salt-and-pepper noise was generated at densities ranging from 10% to 90%, where corrupted pixels were randomly assigned values 0 (pepper) or 255 (salt). For each noise level, five independent noise realizations were generated, and the average PSNR, MSE, and SSIM values were reported. Experiments were performed on standard grayscale test images such as Lena, Barbara, lake, boat and living room. The Figures 2 used in this study include: (a) Lenna, (b) Barbara, (c) lake, (d) boat, and (e) living room shown in Figures 2(a)-(e).

(a) (b) (c)

(d) (e)

Figure 2. Five sample images: (a) Lenna, (b) Barbara, (c) lake, (d) boat, and (e) living room

4.2. Quantitative performance

The qualitative analysis of the proposed technique is presented here. Figure 3 illustrates the performance of the proposed filtering approach on the Lenna image. The upper images depict noisy versions of the image with salt-and-pepper noise levels ranging from 10(100) to 30(100), representing different levels of noise corruption. The lower images showcase the results after applying the proposed denoising method. As the noise density increases, conventional filters often struggle to retain structural details, leading to blurring and loss of fine textures. However, the proposed method significantly improves image clarity while preserving edges and fine details, as evident in the lower images. This observation is quantitatively supported by PSNR and SSIM measurements, which demonstrate superior noise removal and structural preservation compared to traditional filtering techniques. The method effectively suppresses severe salt-and-pepper noise while preserving key image features, supporting its use in optical image enhancement.

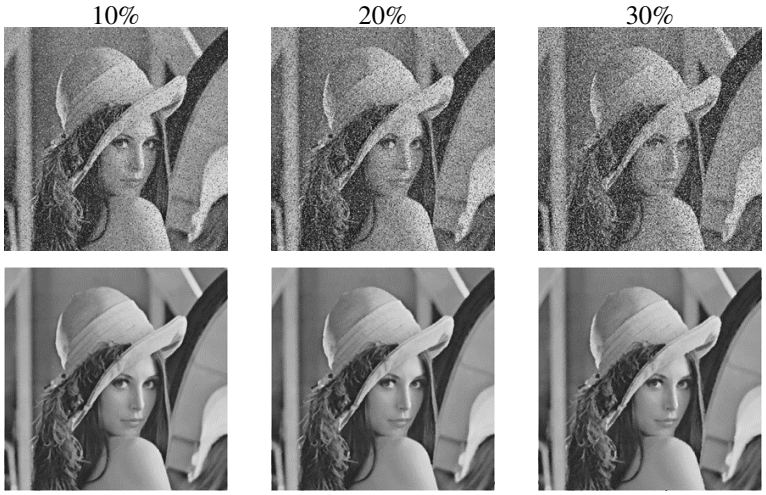

Figure 3. The results of the proposed filtering technique for Lenna images

Figure 4 illustrates, as the noise density increases, the effectiveness of traditional filtering methods diminishes, leading to more visible noise artifacts. In contrast, the proposed method maintains image quality with significantly fewer distortions.

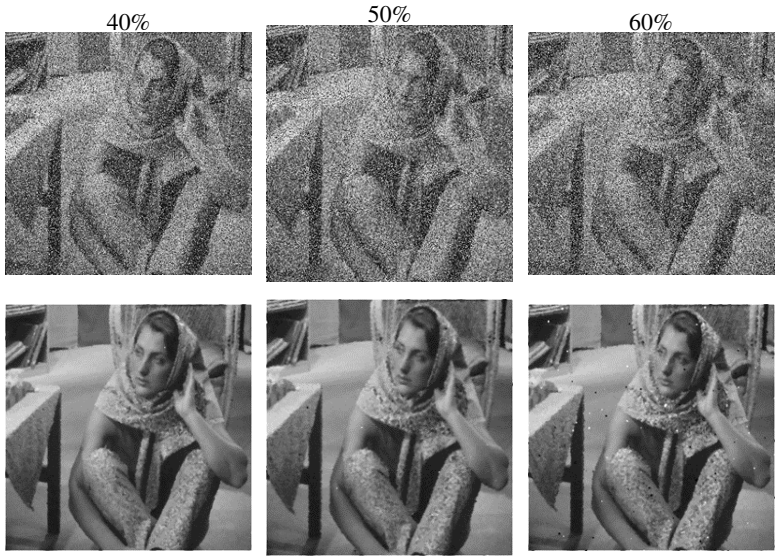

Figure 4. The results of the proposed filtering technique for Barbara images

The filtering outcomes for the Lake image are shown in Figure 5, where noisy images with salt-and-pepper noise levels ranging from 70% to 90% were processed. The proposed method significantly reduced noise, leading to improved edge definition and reduced distortion artifacts. In high noise conditions (above 80%), traditional median-based filters fail to accurately reconstruct edges, often resulting in over-smoothing. However, the proposed method demonstrated stronger edge retention, as confirmed by SSIM and MSR values, which indicated that the filtered images had higher structural similarity and lower residual error compared to median filtering. These improvements highlight the ability of the proposed method to suppress high-density noise while preserving fine structural details, making it more effective than conventional denoising approaches.

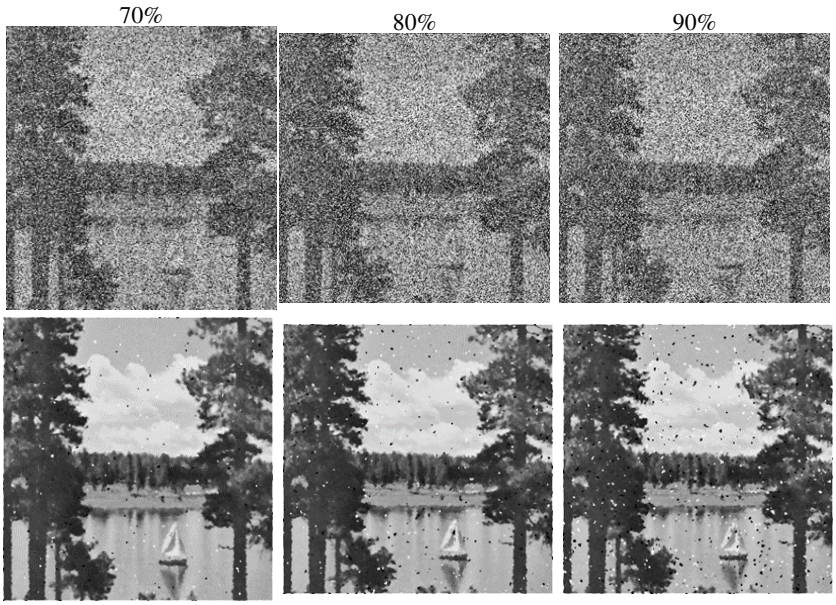

Figure 5. The results of the proposed filtering technique for lake images

Quantitative analysis of the image filtering results is summarized in Table 2. showing improvements across all metrics. Among them, SSIM offers a more perceptually meaningful assessment compared to MSE and PSNR, as the latter quantify absolute errors while SSIM accounts for structural and saliency-based differences. As noise density rises, output image quality decreases, as illustrated in Figure 6, which compares MSE values for noise levels of 10%, 20%, and 30%. The x-axis denotes noise density across five test images, while the y-axis shows the corresponding MSE.

Table 2. Image quality metrics results of the proposed method

Images	Noise	MSE	SSIM	PSNR
	0.1	8.89	37.55	0.9950
Lenna	0.2	9.10	37.44	0.9948
	0.3	9.36	38.41	0.9950
	0.1	10.05	37.24	0.9936
Barbara	0.2	10.19	37.18	0.9933
	0.3	10.36	37.97	0.9935
	0.1	9.17	38.50	0.9951
Lake	0.2	9.66	38.27	0.9949
	0.3	9.75	38.23	0.9947
	0.1	7.76	38.95	0.9945
Boat	0.2	7.85	38.90	0.9943
	0.3	8.17	39.00	0.9940
	0.1	8.26	38.95	0.9939
Living Room	0.2	8.38	38.89	0.9936
	0.3	8.75	38.70	0.9933

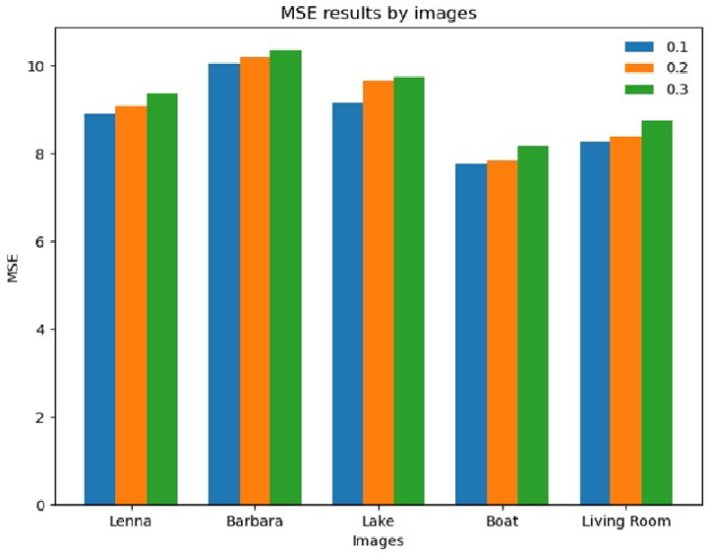

Figure 6. Graph of the MSE

The proposed method's performance, assessed using MSE, demonstrates superior results relative to conventional filtering approaches over various noise densities, with consistently lower MSE values. Although MSE gradually increases with higher noise levels, the method effectively preserves image quality even under severe corruption, as indicated in Table 3 and Figure 7 illustrates the MSE variation across different noise densities. The x-axis represents noise density, while the y-axis represents MSE values. The figure highlights how the proposed method consistently outperforms traditional filters in reducing mean squared error.

Table 3. A comparison of MSE average values

Noise	10%	20%	30%	40%	50%
Mean Filter	28.12	51.23	74.23	94.32	109.21
Median Filter	28.52	52.33	78.22	98.23	112.23
Gaussian Filter	26.11	52.10	75.23	94.09	108.12
Proposed Filter	8.826	9.10	10.36	10.48	11.12

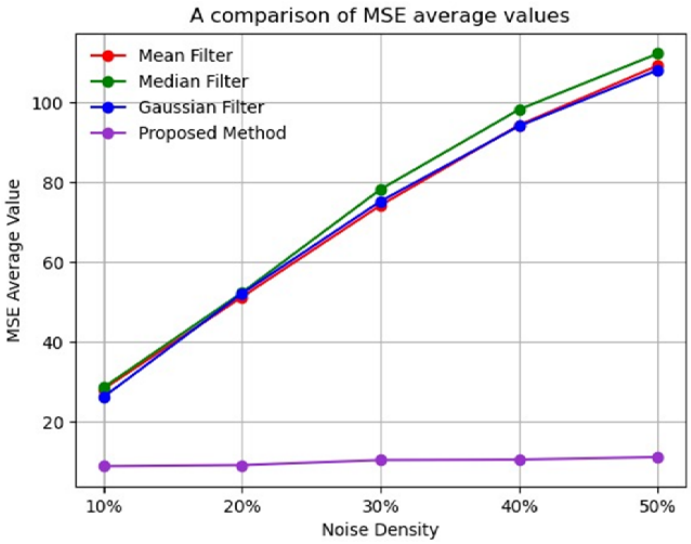

Figure 7. Graph of a comparison of MSE with different techniques

The proposed filtering approach outperforms traditional methods across various noise densities. The average PSNR values for the proposed technique are consistently higher than those of the median, modified decision based unsymmetric trimmed median filter (MDBUTMF) and based on pixel density filter (BPDF) [11]. At 10% noise density, the PSNR for the proposed method is 38.23, compared to 28.49 for the median filter, 34.28 for the MDBUTMF, and 35.64 for BPDF. This superior performance is maintained even at higher noise levels, yielding PSNR values of 37.17, 36.88, 34.07, and 31.41 as shown in Table 4. Figure 8 presents the PSNR comparison at different noise levels. The x-axis represents noise density, while the y-axis represents PSNR values. The graph includes legends distinguishing between median filter, MDBUTMF, based on BPDF and the proposed method.

Table 4. Comparing PSNR average values

Noise	10%	30%	50%	70%	90%
MDBUTMF	34.28	29.89	27.53	25.63	21.78
Median filter	28.49	26.06	22.23	16.45	8.98
BPDF	35.64	29.76	25.87	21.42	10.62
Proposed filter	38.23	37.17	36.88	34.07	31.41

Figure 8 graph of a comparing PSNR average values for various techniques for filtering. This study compares various filtering methods for suppressing salt-and-pepper noise in digital images. Using SSIM as the quality metric, the proposed method outperforms other methods across various noise densities. The study shows better improvement in SSIM over the baseline median filter, contributing to the existing research on effective image denoising techniques. The proposed filter achieves an SSIM of 0.99 at a 10% noise level, surpassing conventional methods such as the median filter, MDBUTMF, and BPDF [11]. As the noise density rises, the performance advantage becomes more pronounced, with the filter maintaining an SSIM of 0.98 even at 30%, as summarized in Table 5.

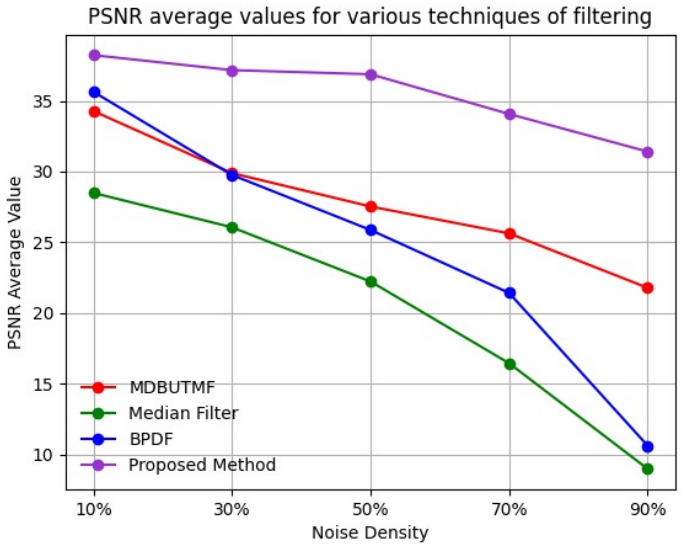

Figure 8. Graph of a comparing PSNR average values for various techniques for filtering

Table 5. Comparison of SSIM average values for several filtering methods

Noise	10%	30%	50%	70%	90%
MDBUTMF	0.97	0.91	0.85	0.76	0.59
Median Filter	0.82	0.76	0.63	0.36	0.05
BPDF	0.98	0.95	0.91	0.87	0.82
Proposed Filter	0.99	0.98	0.97	0.96	0.94

Figure 9 illustrates SSIM variations across different noise levels, with the x-axis representing noise density and the y-axis indicating SSIM values. The legend distinguishes among the filtering techniques, highlighting the proposed method's ability to preserve structural similarity at high noise densities. This enhanced performance stems from its capability to accurately differentiate between noisy and clean pixels, enabling precise noise suppression without compromising image details-an advantage over traditional spatial-domain filtering methods.

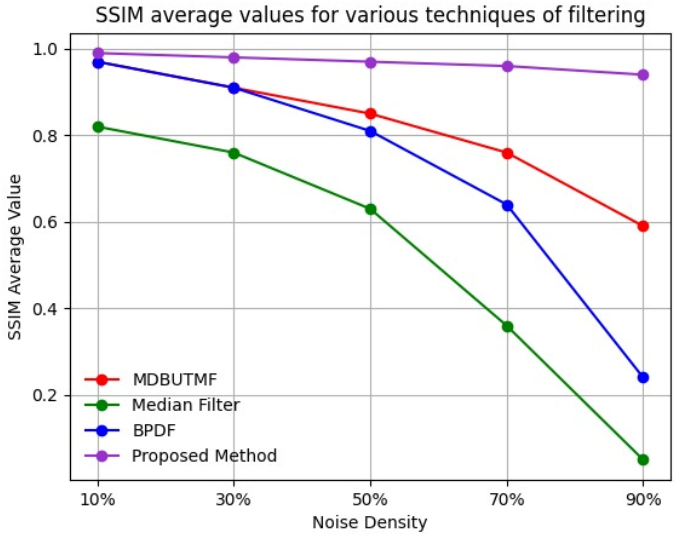

Figure 9. Graph of a comparing SSIM average values for various techniques for filtering

4.3. Limitations and discussion

Although the proposed method exhibits superior robustness, several limitations must be noted,

- Extremely high noise densities (90%)
  When more than 90% of the pixels in a 3×3 window is corrupted, quartile estimation becomes unstable and the median loses representativeness. This limitation is inherent to window-based statistical filtering approaches.
- Fine texture sensitivity
  Small natural intensity variations in textured regions can result in a narrow inter-quartile range, which may lead to mild over-smoothing in localized areas.
- Computational cost
  The method is more computationally expensive than simple median filtering due to sorting and statistical evaluation, but significantly faster than PDE-based or learning-based models.
- Fixed kernel size
  A fixed 3 × 3 window provides effective performance for most test images;however, multi-scale strategies may be more suitable for images containing large homogeneous regions.
- Sharpening parameter dependence
  Fixed sharpening weights work well for natural images but may require tuning for medical or low-light imaging.
- Noise-type specificity
  The method is optimized for salt-and-pepper noise. Mixed-noise conditions represent a future direction.

4.4. Overall discussion

Despite these limitations, the proposed method consistently outperforms classical and decision-based approaches at all noise densities, particularly under extreme corruption conditions. This confirms the effectiveness of the dual-layer design and its suitability for real-world impulsive noise scenarios.

5. CONCLUSION

This paper presented a robust dual-layer denoising framework for removing high-density salt-and-pepper noise from grayscale images. The proposed method combines rank-4 prescreening with adaptive IQR-based outlier detection using Tukey fences, followed by a sharpening and smoothing stage to restore structural details. The integration of rank statistics and quartile-based boundaries enables reliable noise detection even when most pixels within a local 3×3 neighborhood are corrupted, a condition under which many existing filters fail. Experimental results across noise densities from 10% to 90% demonstrate that the proposed approach consistently achieves higher PSNR, lower MSE, and superior SSIM compared with classical median-based filters and state-of-the-art decision-based methods such as BPDF and MDBUTMF. Although performance gradually degrades beyond extremely high noise levels exceeding 90%, this limitation is inherent to local window-based statistical filtering. The algorithm remains computationally efficient due to its fixed window size and simple statistical operations, making it practical for real-world applications. Overall, the proposed dual-layer framework offers a statistically guided and effective solution for extreme salt-and-pepper noise removal. Future work may focus on adaptive multi-scale windowing, automatic tuning of sharpening parameters, and extensions to mixed-noise scenarios involving Gaussian, Poisson, or speckle noise.

ACKNOWLEDGEMENT

The authors would like to thank the reviewers for their insightful comments and valuable suggestions, which significantly improved the quality of this manuscript.

FUNDING INFORMATION

This research received no external funding.

AUTHOR CONTRIBUTIONS

This journal uses the Contributor Roles Taxonomy (CRediT) to recognize individual author contributions, reduce authorship disputes, and facilitate collaboration.

Name of Author	C	M	So	Va	Fo	I	R	D	O	E	Vi	Su	P	Fu
Ali Salem Al Rawash	✓	✓	✓		✓	✓		✓	✓	✓				✓
Farah Aini Abdullah		✓		✓	✓						✓	✓	✓	✓
Ahmad Kadri Junoh	✓	✓	✓	✓	✓		✓				✓	✓	✓	
Abdallah Alshbeel						✓				✓				✓
Mohammed Banikhalid						✓								✓

C : **C**onceptualization
M : **M**ethodology
So : **So**ftware
Va : **Va**lidation
Fo : **Fo**rmal Analysis
I : **I**nvestigation
R : **R**esources
D : **D**ata Curation
O : Writing - **O**riginal Draft
E : Writing - Review & **E**diting
Vi : **Vi**sualization
Su : **Su**pervision
P : **P**roject Administration
Fu : **Fu**nding Acquisition

CONFLICT OF INTEREST STATEMENT

The authors declare that there is no conflict of interest regarding the publication of this paper.

DATA AVAILABILITY

The datasets used in this study are publicly available from standard image processing benchmark databases (e.g., Lenna, Barbara, Boat, Lake, and Living Room). Additional data supporting the findings of this study are available from the corresponding author upon reasonable request.

REFERENCES

[1] D. Kusnik and B. Smolka, "Robust mean shift filter for mixed Gaussian and impulsive noise reduction in color digital images," *Scientific Reports*, vol. 12, no. 1, p. 14951, 2022, doi: 10.1038/s41598-022-19161-0.

[2] X. Wang, T. Chen, D. Li, and S. Yu, "Processing methods for digital image data based on the geographic information system complexity," *Complexity*, vol. 2021, Art. no. 2319314, 2021. doi: 10.1155/2021/2319314.

[3] U. Yuandari, "Improving the quality of digital images using the image averaging method," *The IJICS (International Journal of Informatics and Computer Science)*, vol. 4, no. 1, pp. 5-11, 2020, doi: 10.30865/ijics.v4i1.1982.

[4] R. Al-taie, B. Saleh, and H. Abu-Alsaad, "A review paper digital image filtering processing," *Technium: Romanian Journal of Applied Sciences and Technology*, vol. 3, no. 9, pp. 1–11, 2021, doi: 10.47577/technium.v3i9.4913.

[5] S. K. Satpathy, S. Panda, K. K. Nagwanshi, S. K. Nayak, and C. Ardil, "Adaptive non-linear filtering technique for image restoration," *International Journal of Computer and Information Engineering*, vol. 16, no. 4, pp. 154-161, 2022 (Originally arXiv:2204.09302).

[6] N. Kumar, A. K. Dahiya, and K. Kumar, "Modified median filter for image denoising," *International Journal of Advanced Science and Technology*, vol. 29, no. 4, pp. 1495–1502, 2020.

[7] B. A. Bello, M. A. Bagiwa, A. D. Kana, and M. Abdullahi, "An improved connectivity-based outlier factor median filter (ICOFMED)," *Proceedings of the International Conference on Computing and Advances in Information Technology (ICCAIT)*, 2023.

[8] B. Goyal, A. Dogra, S. Agrawal, and B. S. Sohi, "A survey on the image denoising to enhance medical images," *Biosciences Biotechnology Research Asia*, vol. 15, no. 3, pp. 501–507, 2018, doi: 10.13005/bbra/2655.

[9] O. Joshua, J. S. Owotogbe, T. S. Ibiyemi, and B. A. Adu, "A comprehensive review on various types of noise in image processing," *International Journal of Scientific and Engineering Research*, vol. 10, no. 11, pp. 364-370, 2019.

[10] S. Yadav, D. S. Taterh, and M. A. Saxena, "A literature review of various techniques available on Image Denoising," *International Journal of Engineering, Business and Management*, vol. 5, no. 2, pp. 1–7, 2021, doi: 10.22161/ijebm.5.2.1.

[11] U. Erkan and L. Gokrem, "A new method based on pixel density in salt and pepper noise removal," *Turkish Journal of Electrical Engineering and Computer Sciences*, vol. 26, no. 1, pp. 162–171, 2018, doi: 10.3906/elk-1705-256.

[12] L. Fan, F. Zhang, H. Fan, and C. Zhang, "Brief review of image denoising techniques," *Visual Computing for Industry, Biomedicine, and Art*, vol. 2, no. 1, p. 7, 2019, doi: 10.1186/s42492-019-0016-7.

[13] IEEE Publication Technology, "RGB-thermal based denosing methods a review of deep learning based image denosing algorithm and application", *Journal of Latex Class Files*, Vol. 14, No. 8, pp. 1–35, 2021.

[14] A. Shah, J. I. Bangash, A. W. Khan, I. Ahmed, A. Khan, A. Khan, and A. Khan, "Comparative analysis of median filter and its variants for removal of impulse noise from gray scale images," *Journal of King Saud University - Computer and Information Sciences*, vol. 34, no. 3, pp. 505–519, 2022, doi: 10.1016/j.jksuci.2020.03.007.

[15] A. Prasetio and P. M. Hasugian, "Improving the quality of digital images using the median filter technique to reduce noise," *SinkrOn: Jurnal dan Penelitian Teknik Informatika*, vol. 4, no. 1, pp. 143-147, 2019.

[16] B. R. Jana and J. Beatrice Seventline, "A modified trimmed median filter technique for noise removal in an image," *International Journal of Innovative Technology and Exploring Engineering*, vol. 8, no. 6S4, pp. 583–586, 2019.

[17] Y. Lotfi and K. Parand, "Efficient image denoising technique using the meshless method: Investigation of operator splitting RBF collocation method for two anisotropic diffusion-based PDEs," *Computers and Mathematics with Applications*, vol. 113, pp. 315-331, 2022.

[18] J. Yang, S. Rahardja, and P. Franti, "Mean-shift outlier detection and filtering," *Pattern Recognition*, vol. 115, p. 107874, 2021.

[19] S. Rani, Y. Chabbra, and K. Malik, "An improved denoising algorithm for removing noise in color images," *Engineering, Technology and Applied Science Research*, vol. 12, no. 3, pp. 8738–8744, 2022, doi: 10.48084/etasr.4952.

[20] M. Abu-Faraj, A. Al-Hyari, B. Al-Ahmad, Z. Alqadi, A. Ali, and K. Aldebe, "Improving the efficiency of median filters using special generated windows," *Applied Mathematics and Information Sciences*, vol. 17, no. 1, pp. 187–200, 2023, doi: 10.18576/amis/170119.

[21] N. Cao and Y. Liu, "High-noise grayscale image denoising using an improved median filter for the adaptive selection of a threshold," *Applied Sciences*, vol. 14, no. 2, p. 635, 2024, doi: 10.3390/app14020635.

[22] T. M. Alanazi, K. Berriri, M. Albekairi, A. Ben Atitallah, A. Sahbani, and K. Kaaniche, "New real-time high-density impulsive noise removal method applied to medical images," *Diagnostics*, vol. 13, no. 10, p. 1709, 2023, doi: 10.3390/diagnostics13101709.

[23] U. Erkan, D. N. H. Thanh, L. M. Hieu, and S. Enginoglu, "An iterative mean filter for image denoising," *IEEE Access*, vol. 7, pp. 167847–167859, 2019, doi: 10.1109/ACCESS.2019.2953924.

[24] U. Erkan, S. Enginoglu, D. N. H. Thanh, and L. M. Hieu, "Adaptive frequency median filter for the salt and pepper denoising problem," *IET Image Processing*, vol. 14, no. 7, pp. 1240–1247, 2020, doi: 10.1049/iet-ipr.2019.0398.

[25] A. Abdurrazzaq, A. K. Junoh, W. Z. A. W. Muhamad, Z. Yahya, and I. Mohd, "An overview of multi-filters for eliminating impulse noise for digital images," *Telecommunication Computing Electronics and Control (TELKOMNIKA)*, vol. 18, no. 1, pp. 343-349, 2020.

[26] F. Chen, ,M. Huang, Z. Ma, Y. Li, Q. Huang, "An iterative weighted-mean filter for removal of high-density salt-and-pepper noise", *Symmetry*, vol. 12, no. 12, pp. 1-12, 1990, doi: 10.3390/sym12121990.

[27] S. Ma, L. Li, and C. Zhang, "Adaptive image denoising method based on diffusion equation and deep learning," *Journal of Robotics*, vol. 2022, Art. no. 7977755, 2022.

[28] S. M. Kaddour, M. Lehsaini, and A. Bouchachia, "Event detection for non-intrusive load monitoring using Tukey's fences," *arXiv preprint arXiv:2402.17809*, 2024.

[29] Y. Jiang, H. Wang, Y. Cai, and B. Fu, "Salt and pepper noise removal method based on the edge-adaptive total variation model," *Frontiers in Applied Mathematics and Statistics*, vol. 8, p. 918357, 2022, doi: 10.3389/fams.2022.918357.

[30] L. Han, Y. Zhao, H. Lv, Y. Zhang, H. Liu, and G. Bi, "Remote sensing image denoising based on deep and shallow feature fusion and attention mechanism," *Remote Sensing*, vol. 14, no. 5, p. 1043, 2022, doi: 10.3390/rs14051043.

BIOGRAPHIES OF AUTHORS

Ali Salem Al Rawash received his Bachelor's degree in Mathematics from Al al-Bayt University, Jordan. He later completed his Master's degree in Mathematics at Universiti Malaysia Perlis (UniMAP), Malaysia, and is currently pursuing a Ph.D. in Mathematics at Universiti Sains Malaysia (USM). His academic journey reflects a consistent dedication to mathematical research and higher education. Ali has accumulated valuable teaching experience across several educational institutions, including secondary schools and universities, where he has taught a wide range of mathematical subjects. His research interests include image processing, mathematical modeling, partial differential equations, and applied linear algebra. In his current doctoral research, he focuses on developing robust noise removal algorithms for grayscale images using outlier detection and singular value decomposition techniques. His contributions aim to enhance image quality preservation in digital imaging applications. Ali is committed to advancing knowledge in applied mathematics and fostering educational excellence through research and teaching. He can be contacted at email: alisalem@student.usm.my.

Farah Aini Abdullah Assoc. Prof. Dr. Farah Aini Abdullah completed her Ph.D. in Computational Mathematics from The University of Queensland in 2009. Since graduation, she has worked in computational and applied mathematics at the School of Mathematical Sciences, Universiti Sains Malaysia, 11800 USM, Pulau Pinang, Malaysia. Dr. Farah Aini has also been appointed as an Adjunct Associate Professor (1-year duration from October 2025 until Sept 2026) for the Nonlinear Dynamics Research Center (NDRC), Ajman University, Ajman, UAE. She is interested in the fields of computational mathematics, computational biology, and fractional differential modeling. Currently, her research project is on fractional dynamical models arising from biological/epidemiological problems. She can be contacted at email: farahaini@usm.my.

Ahmad Kadri Junoh is an associate professor at the Faculty of Intelligent Computing, Universiti Malaysia Perlis (UniMAP) Arau, Perlis, Malaysia. He earned a B.Eng (Mechanical) from Akita University, Japan; a M.Sc. in Mathematics; and a Ph.D. in Mechanical and Materials Engineering from Universiti Kebangsaan Malaysia. His research domains are artificial intelligence, data science and applied mathematics, with several Scopus-and ISI-indexed publications. He supervises postgraduate students, including Ph.D. candidates, and contributes actively to academic life and community engagement. He can be contacted by email kadri@unimap.edu.my.

Abdallah Alshbeel is a Ph.D candidate at the School of Mathematical Sciences, Universiti Sains Malaysia (USM). He majored in mathematics during his master's studies. He has been working on research related to applied mathematics. He can be contacted at email: abdallahalshbeel@student.usm.my.

Mohammed Banikhalid is currently pursuing a Ph.D. in Mathematics at Universiti Sains Malaysia (USM). He has published research papers in peer-reviewed journals in the field of partial differential equations. He holds a Bachelor's degree from The Hashemite University and an M.Sc. from Irbid National University, both in Mathematics. He has presented his work at international conferences in Turkey and Greece, and previously taught Mathematics at King Saud University. He can be contacted at email: mohammedbanikhalid@student.usm.my.